High-Frequency Signature-Based Fault Detection for Future MV Distribution Grids

Preprint

Yaswanth Nag Velaga,[1] Kumaraguru Prabakar,[1] Akanksha Singh,[1] and Pankaj K. Sen[2]

1 National Renewable Energy Laboratory
2 Colorado School of Mines

Presented at the 56th IEEE Industrial and Commercial Power Systems Technical Conference (I&CPS)
June 29–July 28, 2020

NREL is a national laboratory of the U.S. Department of Energy
Office of Energy Efficiency & Renewable Energy
Operated by the Alliance for Sustainable Energy, LLC

This report is available at no cost from the National Renewable Energy Laboratory (NREL) at www.nrel.gov/publications.

Contract No. DE-AC36-08GO28308

Conference Paper
NREL/CP-5D00-74785
July 2020

High-Frequency Signature-Based Fault Detection for Future MV Distribution Grids

Preprint

Yaswanth Nag Velaga,[1] Kumaraguru Prabakar,[1] Akanksha Singh,[1] and Pankaj K. Sen[2]

1 National Renewable Energy Laboratory
2 Colorado School of Mines

Suggested Citation
Velaga, Yaswanth Nag, Kumaraguru Prabakar, Akanksha, Singh, and Pankaj K. Sen. 2020. *High-Frequency Signature-Based Fault Detection for Future MV Distribution Grids: Preprint*. Golden, CO: National Renewable Energy Laboratory. NREL/CP-5D00-74785. https://www.nrel.gov/docs/fy20osti/74785.pdf.

NREL is a national laboratory of the U.S. Department of Energy
Office of Energy Efficiency & Renewable Energy
Operated by the Alliance for Sustainable Energy, LLC

This report is available at no cost from the National Renewable Energy Laboratory (NREL) at www.nrel.gov/publications.

Contract No. DE-AC36-08GO28308

Conference Paper
NREL/CP-5D00-74785
July 2020

National Renewable Energy Laboratory
15013 Denver West Parkway
Golden, CO 80401
303-275-3000 • www.nrel.gov

NOTICE

This work was authored by the National Renewable Energy Laboratory, operated by Alliance for Sustainable Energy, LLC, for the U.S. Department of Energy (DOE) under Contract No. DE-AC36-08GO28308. Funding provided by U.S. Department of Energy Office of Energy Efficiency and Renewable Energy Solar Energy Technologies Office Agreement Number 34237. The views expressed herein do not necessarily represent the views of the DOE or the U.S. Government.

High-Frequency Signature-Based Fault Detection for Future MV Distribution Grids

Yaswanth Nag Velaga*, Kumaraguru Prabakar*, Akanksha Singh*, and Pankaj K. Sen†
*Power Systems Engineering Center, National Renewable Energy Laboratory, Golden, Colorado
†Department of Electrical Engineering, Colorado School of Mines, Golden, Colorado

***Abstract*—Increasing penetration levels of inverter based distributed energy resources (DERs) impact the legacy distribution system protection. Inverter based DERs provide approximately 1.2-2 pu fault current. In systems with high penetration of inverter based DERs, it is difficult for over-current based protection schemes to differentiate between normal loading conditions and a fault. Directional, distance, and adaptive forms of protection schemes are also affected by low fault currents. This paper analyzes fault generated traveling wave (TW) based high-frequency signatures in the distribution system. In order to simulate such signatures, frequency-dependent distributed parameter line modeling approach is used in this research work to represent distribution lines and underground cables. Modified IEEE 13-bus medium voltage test system is modeled in electromagnetic transient simulation tool and multiple transient scenarios are simulated in this test system. The results are analyzed to understand the high-frequency signatures that can be used to detect and locate faults under high penetration of DERs.**

***Keywords*—Distribution line modeling, distribution system protection, electromagnetic transient program, EMTP, fault analysis, fault detection, high-frequency signature, traveling wave.**

I. Introduction

Increasing penetration levels of distributed energy resources (DERs) in distribution network may cause bi-directional power flow and raise several challenges in system operations such as protection, voltage rise, frequency control, and stability [1]. Out of these, protection requires special attention because it can restrict and limit the expansion and penetration level of DERs. Traditional synchronous generators generally contribute a significant amount of fault current: approximately 6-10 times the rated generator current. Existing overcurrent (OC) schemes utilize this large fault current to distinguish between normal and fault condition.

Inverter based DERs, unlike rotating machines, lack the inertia and contribute about 1-2 pu fault current [2]. This fault current contribution also varies depending on system configuration and operating conditions. As DER penetration increases, the existing OC fault protection schemes may fail due to bi-directional power flow. These protection issues are discussed in [3]. Additionally, fault ride-through capabilities of DERs, that are defined in the interconnection standard [4], create additional challenges for existing protection schemes.

Recent studies have proposed multiple approaches to address these issues. A directional overcurrent protection scheme with communications links to all protective devices based on the IEC 61850 substation automation system is proposed in [5]. But, directional feature is not reliable for close-in faults because of voltage collapse on faulted phases [6]. Furthermore, the directionality of single-line-to-ground (SLG) faults is difficult to detect because of the existence of multiple ground sources in a distribution system. Also, installation of potential transformers, current transformers, and communications at every node will be expensive.

Distance based protection schemes provide inherent directionality with fixed reach and are independent of changing system conditions [7]. They are affected by outfeed of tap load currents and infeed from generation sources between the fault and relay, which makes these schemes over-reach and under-reach. Distance protection is also not reliable for detecting high-resistance faults and reverse close-in faults. Additionally, changing grid conditions make it difficult to find the optimal relay settings. And applying such distance based protection schemes to a distribution system with DERs is challenging. To account for changes in system topology, such as grid-connected and islanded operation, the adaptive protection scheme has gained traction in recent years [8]–[13]. Typically, centralized control detects the network status and updates the device settings over a communications link. But, they are expensive and practical difficulties are associated with their implementation [14].

The future distribution system with high penetration of inverter based DERs requires innovative protection schemes that can handle variable fault current, bi-directional power flow, and changing system conditions, etc. This paper proposes the traveling wave (TW) based high-frequency signatures for medium voltage (MV) distribution system protection. When a fault occurs, a very high-frequency voltage and current waves are generated at the fault point. These waves are independent of the type of fault, topology of the system, and location of the fault. In transmission system, transients caused by the faults contain energy over a broad frequency spectrum, between 20 kHz and 2 MHz [15]. There are many challenges to design a protection scheme based on TWs because of their behavior

This work was authored by the National Renewable Energy Laboratory, operated by Alliance for Sustainable Energy, LLC, for the U.S. Department of Energy (DOE) under Contract No. DE-AC36-08GO28308. This material is based upon work supported by the U.S. Department of Energy's Office of Energy Efficiency and Renewable Energy (EERE) under Solar Energy Technologies Office (SETO) Agreement Number 34237. The views expressed in the article do not necessarily represent the views of the DOE or the U.S. Government. The U.S. Government retains and the publisher, by accepting the article for publication, acknowledges that the U.S. Government retains a nonexclusive, paid-up, irrevocable, worldwide license to publish or reproduce the published form of this work, or allow others to do so, for U.S. Government purposes.

across different components in the system.

A study in [16], proposed a single line-to-ground (SLG) fault travelling wave based protection for less effective grounded systems. A simplified 35 kV radial distribution system is used. Authors did not analyze the effect of transformers and capacitors which are predominantly found in distribution. Similarly, the authors in [17] discussed using the protection scheme on medium voltages to detect the direction and location using only current measurements. The authors assumed that the lines were homogeneous with no discontinuities and reflections. Because of the presence of a wide-frequency band in the generated waves, TWs in the distribution system are referred to as high-frequency waves (HFW).

The rest of this paper is organized as follows. Section II briefly discusses the challenges to using TWs in the distribution system. Section III discusses the importance of selecting the appropriate line models that can be used in the system transient model and provides a comparison among the available models. Section IV discusses the modeling of a modified IEEE 13-bus distribution system in EMTP-RV without transformers to understand the TW behavior in distribution systems and presents different simulation cases and results by varying the location of the faults and fault type.

II. High-Frequency Transients in Distribution Systems

Faults on a distribution line generate surges that propagate in the form of HFWs at finite velocity along the line from the fault location. The propagation velocity, characteristic impedance and the wave shape of these HFWs depend on the line parameters: resistance (R), inductance (L), capacitance (C), and conductance (G). Generally, line parameters are distributed and depend on the physical aspects of the line design, such as tower geometry, type of conductor, conductor spacing, shield wire, and insulator type. Fig. 1 shows the equivalent circuit of a single conductor line of length Δx.

Consider the simple system shown in Fig. 2 with a overhead line segment of characteristic impedance Z_c between the buses A and B. The line left of bus A has a characteristic impedance Z_d, and the line right of the bus B has a characteristic impedance Z_e. A fault on the line between terminals A-B (as shown in Fig. 2) initiates the wave transients A_i & B_i (Voltage and Current) traveling at approximately speed of light. As the fault generated transients approach the terminals A-B, part of the wave is reflected as A_r & B_r and rest is transmitted as A_t & B_t to the adjacent sections of the terminal. This reflection and transmission of the HFW at the junction (or taps) are caused by the changes in characteristic impedance. These waves also attenuate as they propagate along the line because of losses caused by the line resistance (R) and conductance (G). Attenuation of these waves are greater in distribution systems because of the higher resistance in the lines.

Use of such TWs for fault detection and fault location in transmission system is relatively straightforward by using the characteristics of the line, such as length and impedance. But, compared to a transmission system, there are challenges in using the TW based approach in a distribution network. This is due to the presence of unbalanced short lines, underground cables, transformers, voltage regulators, capacitor banks and

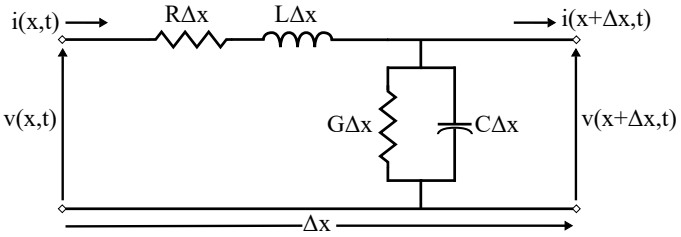

Fig. 1. Equivalent circuit of single-conductor line

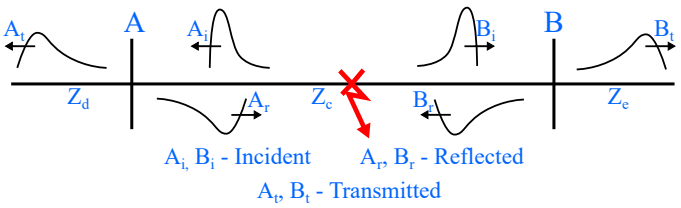

Fig. 2. Illustration of traveling wave at junctions

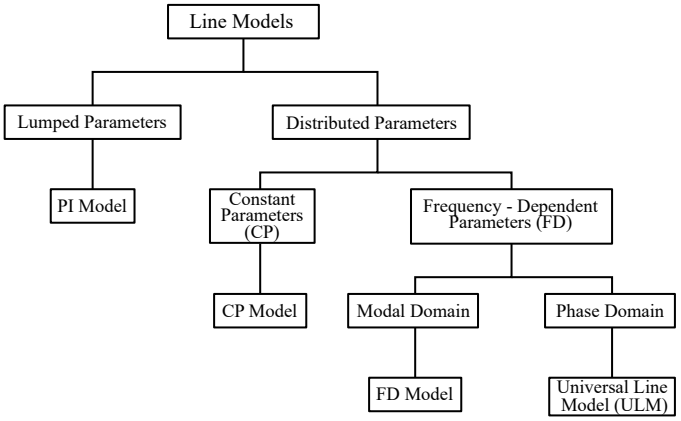

Fig. 3. General classification of line/cable models

frequent taps (point of discontinuities) which can impact TWs in distribution system.

III. Frequency Dependent Line Modeling for Transient Analysis

Accurate representation of the component model is crucial for all transient analyses. Power systems component modeling for electromagnetic transient (EMT) analyses is developed by considering the frequency band of the transients to be analyzed and the frequency dependence of the parameters. Fig. 3 shows the general classification of the line models applicable to overhead lines and underground cables. Line models are divided into two groups: lumped and distributed parameter models. Selecting the model group depends on the highest frequency involved in the study and, to a lesser extent, on the line length.

A. Lumped Parameter Models

Lumped parameter models, also known as pi models, represent the lines and cables by using lumped resistance (R), inductance (L), conductance (G), and capacitance (C) elements. These values are calculated at a single frequency of interest. These models are sufficient for steady-state analysis,

but they can also be used for transient studies provided the parameters are evaluated at the frequency of interest. In some cases, these short pi sections are cascaded to approximate the distributed nature of the line. The number of such sections depends on the expected frequency of the transient [18]. Cascaded pi sections are computationally expensive because of the increase in matrix size. Because pi models do not represent a propagation delay and attenuation of waves, they are best suited for steady-state analysis where high-frequency events are ignored.

B. Distributed Parameter Models

Distributed parameter line models are divided into two sub-groups: constant parameter (CP) and frequency dependent (FD).

1) Constant Parameter Model: A constant parameter or Bergeron's model calculates the line parameters at a single frequency. Then, the calculated line parameters (inductance and capacitance) are distributed. The losses in the line are represented through lumped resistances at three discrete points along the line (1/4 at the both ends, and 1/2 at the middle) [19]. Since the line impedances are constant for the whole range of frequencies in the study, this approach can give inaccurate results if the frequency of the event under study is farther from the frequency used to calculate the parameters. Unless the frequency of the desired transient is known beforehand, the constant parameter model might yield inaccurate results at certain frequencies.

2) Frequency-Dependent Model: The frequency dependent (FD) model has the potential to represent the true nature of the line. Frequency-dependent line/cable models can further be divided into two groups based on the domain in which the frequency-dependent line parameters are evaluated: modal and phase domain.

FD model is a modal domain model that utilizes the transformation matrix to transform from phase to mode and mode to phase quantities. Frequency dependence of line parameters are considered in modal domain. FD model assumes the frequency independent transformation matrix which is constant and real [20]. Accuracy of the FD model is limited to symmetrical or balanced overhead lines because the transformation matrices are frequency dependent for unbalanced lines and cables.

Universal Line Model (ULM) is a phase domain model that works directly in the phase domain by taking the full frequency dependence of line parameters in the form of Characteristic admittance (YC) and the propagation constant (H) matrix transfer functions [21]. ULM models avoids the transformation matrix and simplifying assumptions in the form of modal to phase transformations. This model is highly accurate for any overhead line and underground cable configurations. The ULM model or wide-band model is the best choice for most EMT studies and used in this study.

IV. Test System for High-Frequency Wave Validation

A simple test system that represents the common features of a typical distribution system is necessary to understand the HFWs generated during the transient events. Fig. 4(a) is a modified version of the IEEE 13-bus test distribution system [22]. This modified test system has one feeder operating at 13.8 kV. This feeder runs from the substation for a total length of 4 miles. There are four taps taken off the main feeder to represent real world feeder taps.

Configurations for tower structures, overhead lines, and underground cables used in the test system are based on [23]. The details are presented in Fig. 5. Table I shows the various conductors used in the overhead line configurations. Fig. 5(a), (b), & (c) shows the geometric structure of the overhead lines and conductor spacing. Concentric neutral cable (250 AWG) data taken from [22] is used for the underground cable modeling (shown in Fig. 5(d)). The over head lines, and underground cables in the test networks are modeled using the frequency dependent modeling approach known as Universal Line Model (ULM).

To compare the simulation results with theoretical time taken for the waves to propagate in the lines, alpha mode velocities generated by the ULM model is used to create wave travel time diagram of the test system. This propagation time for HFWs in the test system is shown in Fig. 4(b). Table II shows the single and three phase loads modeled in the test system. Load modelling ensures that the pre-fault current is established in the network steady-state. The source in the test network is modeled as voltage source behind equivalent Thévenin impedance. The impedance values are calculated from fault MVA at power frequency.

V. Simulation of Transient Scenarios for High-Frequency Study

Multiple fault transient scenarios are simulated to characterize the behavior of HFWs in distribution system. The simulations are run at a time step of 100 ns. Faults are applied at 51.83 ms (Phase A voltage peak) after the initialization. Current and voltage probes are installed on every bus and

TABLE I. Overhead Line Data

Node A	Node B	Length(mi)	Phase	Neutral	Spacing ID
			AWG	ACSR	
650	632	1	4/0	1	500
632	633	0.5	1/0	2	505
633	634	0.3	4/0	1	510
632	645	0.5	1/0	2	505
645	646	0.3	4/0	1	510
646	647	0.3	4/0	1	510
632	671A	1	4/0	1	500
671A	671B	1	4/0	1	500
671B	680	1	4/0	1	500
671B	675	0.5	1/0	2	505
671B	684	1	4/0	1	500
684	611	0.3	4/0	1	510
684	692	0.3	4/0	1	510

TABLE II. Test System Load Data

Bus	Type	Real Power (MW)	Reactive Power (MVAR)
647	1-ph	0.1	0.05
634	1-ph	0.1	0.05
692	1-ph	0.03	0.0005
611	1-ph	0.1	0.05
645	3-ph	0.5	0.25
633	3-ph	5	2.5
675	3-ph	0.5	0.1
680	3-ph	2	1

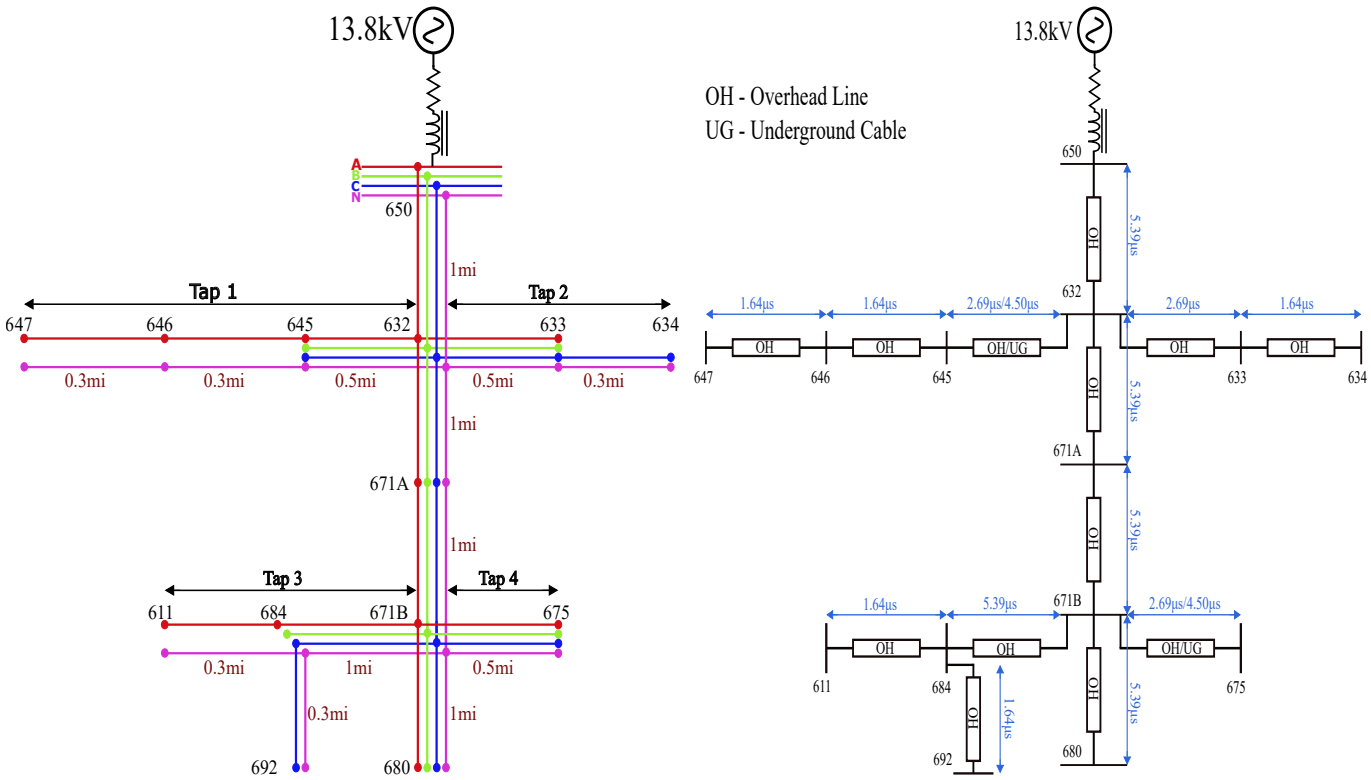

(a) Distribution 13-bus test system

(b) Distribution 13-bus wave travel time

Fig. 4. Modified IEEE test system used in electromagnetic transients simulation

sampled at 10 MHz to record the high-frequency signatures. The signals measured from these probes are filtered through a high-pass filter with a cut-off frequency of 10 kHz. Two fault types, single-line-to-ground (SLG) fault and line-to-line (LL) fault are simulated in two locations. First, on the main feeder. Second, on the tap 1.

A. *Overhead Lines with SLG Fault on Bus 680*

An SLG fault is applied on Phase A at bus 680. Filtered and non-filtered instantaneous values of current and voltage are recorded every 10 μs. All the travel time between buses can be estimated from Fig. 4(b). Filtered signals of all the buses in taps 1 and 3 are plotted to show the arrival times of the waves and compare them with the times shown in Fig. 4(b). The faulted bus current (680) is included in all the plots as a

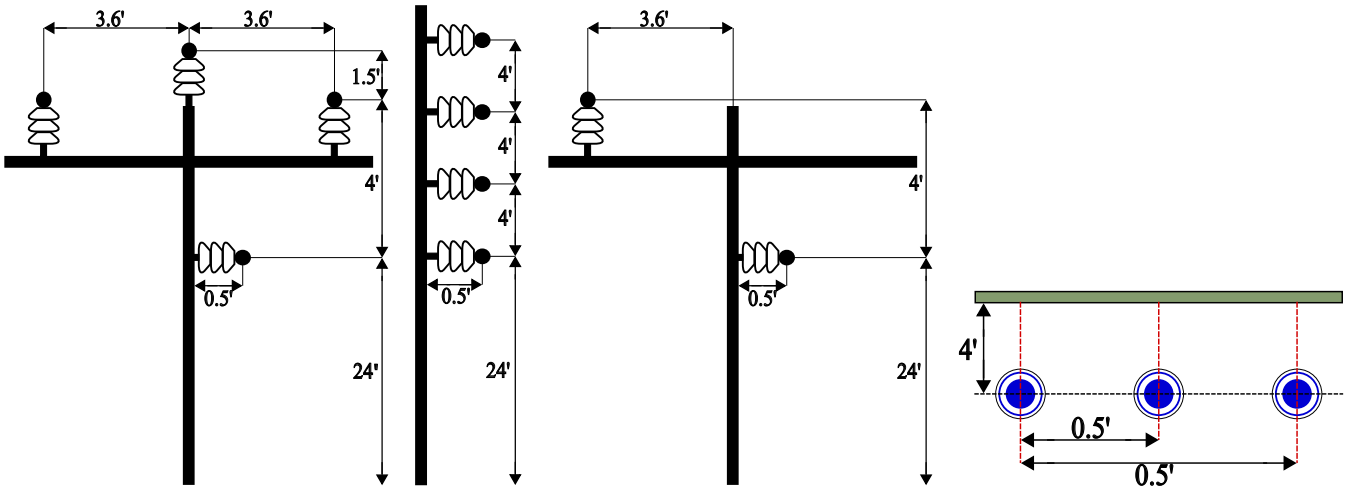

(a) ID-500 (b) ID-505 (c) ID-510 (d) ID-515

Fig. 5. Overhead line tower geometry, and underground cable layout

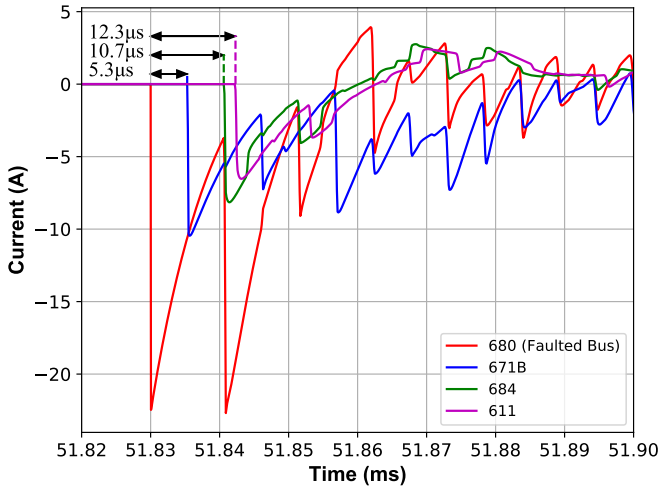

Fig. 6. Filtered currents in tap 3 buses for a SLG Fault

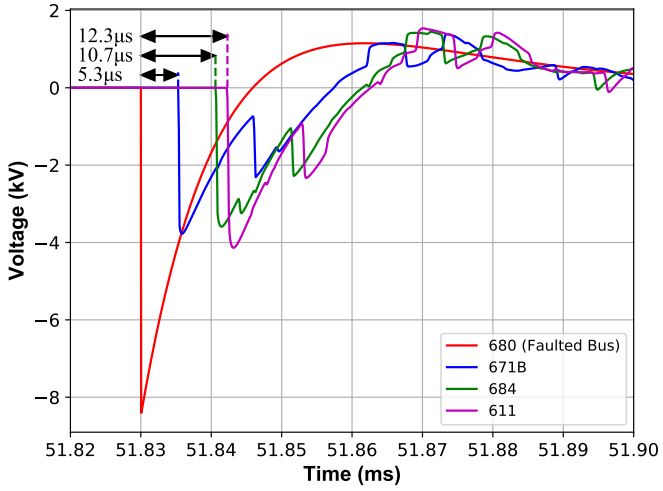

Fig. 7. Filtered voltages in tap 3 buses for a SLG Fault

reference to compare the wave arrival estimates.

High-frequency current wave magnitudes are small due to lower distribution voltage. Current waves are proportional to the voltage wave over characteristic impedance. Voltage and current waves are initiated at the fault point on Phase A at 51.83 ms of simulation time. The current waves propagate and arrive at bus 671B, part of the energy is reflected back and the rest gets split between tap 3, tap 4 and main feeder. Initial current wave times estimated from Fig. 4(b) in tap 3 (671B, 684, 611) are 5.39, 10.78, & 12.42 μs respectively. From the simulations, they arrive at 5.3, 10.7, & 12.3 μs as shown in Fig. 6. Faulted bus 680 records considerably longer duration waves with higher magnitude in Fig. 6, compared to the waves in tap 3. It is because the wave energy attenuates as it travels from fault point and transients recorded at the faulted terminal are always double the magnitude due to same polarity reflections from fault.

Phase to ground instantaneous values of the bus voltages in the tap 3 are shown in Fig. 7. Estimated times of arrival at each bus are estimated the same way as the currents. Voltage and current have the same wave propagation characteristics, so the wave arrival times mentioned in Fig. 6 are applicable to Fig. 7.

Current transients recorded in tap 1 buses are shown in Fig. 8. Signals in tap 2 bus timings are very close to the estimated ones shown in the timing diagram. Comparing the magnitude of the wave that arrived at tap 1 and tap 3 in Fig. 6 and 8, the former is less because of the attenuation in the 2 mi of the main feeder. More taps results in the wave energy getting split at every tap. As the wave attenuates, it also gets distorted in shape, losing its sharp rise characteristic. Initial waves arriving at the bus terminals are always distinct from the system under normal conditions because these wave transients exist only due faults and switching. For faults on the main feeder, any taps that are far away from the fault might not see the measurable reflection from the fault because the energy dissipates in every line between the fault and tap. The closest taps might see the second wave from the fault.

Voltage signals in the tap 1 buses are shown in Fig. 9.

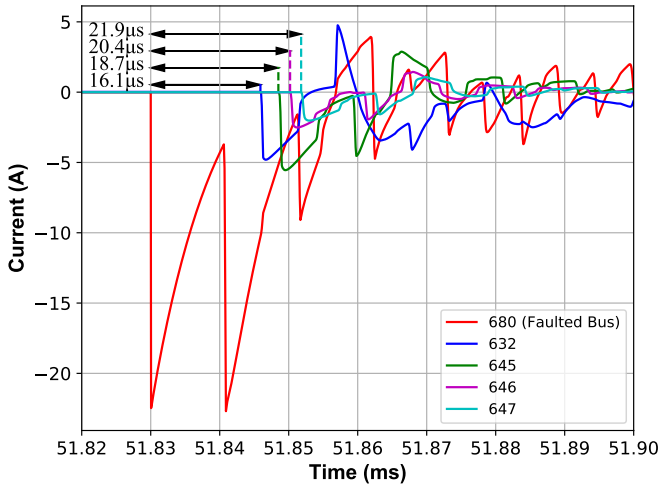

Fig. 8. Filtered currents in tap 1 buses for a SLG Fault

The peak voltage of the traveling wave at bus 632 is about 1.7 kV compared to 4.1 kV at bus 671B. Because the change in characteristic impedance is not great between the bus 632 three-phase and bus 645 single-phase line, most of the wave energy is transmitted to the adjacent line. In distribution systems, different conductors might be used at the same voltage level in a line. Different conductors change the line distributed parameters, but the change in impedance between the adjacent lines is small. Fig. 9 shows that signals in adjacent buses are only displaced in time. A greater difference in characteristic impedance is seen with underground cables in the network.

B. Overhead Lines and Underground Cables with a SLG Fault on Bus 680

Underground cables are mostly used in the distribution systems to serve the densely populated areas. The characteristic impedance of a cable is almost 10 times lower than that of the overhead lines. Wave propagation velocity in a cable is 50-60% of the speed of light due to the insulation permittivity. These crucial differences impact the speed and the attenuation

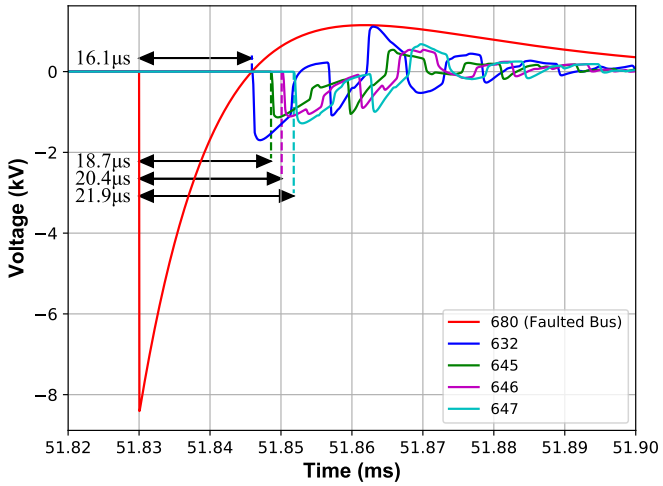

Fig. 9. Filtered voltages in tap 1 for a SLG Fault

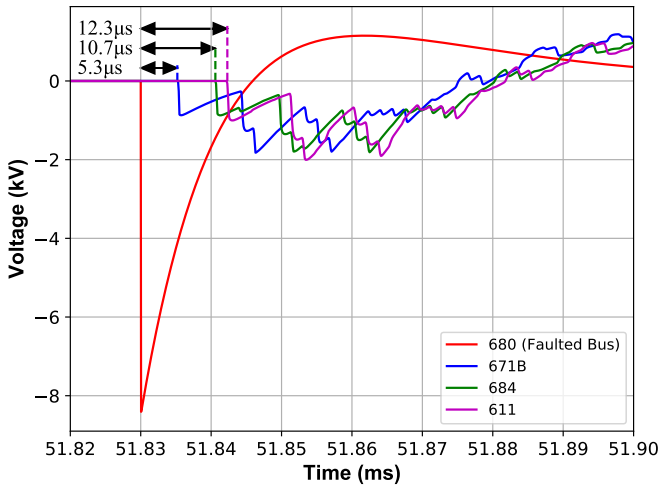

Fig. 10. Filtered voltages in tap 3 buses for a SLG Fault

inside the cables. Understanding and studying these differences between overhead lines and underground cables are critical for creating HFW based protection schemes for systems with overhead lines and underground cables.

In this scenario, two overhead lines between buses 632 and 645, buses 671B and 675 are replaced by a 3-single core cable. Each cable has a central conductor to carry load current and fault current, and an outer sheath to carry ground fault current. Characteristic impedance varies greatly with different cable configurations. Since the characteristics of current and voltage transients are shown to have a same behavior, only voltage waves are used for discussion. First, the voltages in the tap 3 are shown and later comparison between signals at the buses where lines are replaced by cables is made. As seen in Fig. 10. underground cables did not impact the travel time in the overhead lines. Traveling waves are superimposed by an oscillatory signal which frequency is found to be around 8 kHz. High pass filter tuned at 10 kHz attenuated only part of the signal.

The underground cables cause the travel time to increase

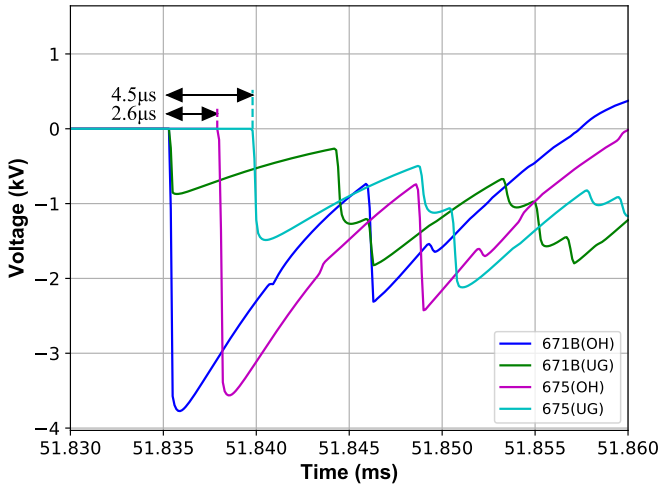

Fig. 11. Voltage wave travel between overhead and underground in tap 4 for a SLG Fault

compared to the overhead line. The travel time through the cable is 4.5 μs, which is same as the simulated time. Voltage signals at bus 671B & bus 675 contain smaller magnitudes of reflections compared to the overhead line as shown in Fig. 11.

C. Overhead Lines with Line-to-Line (LL) Fault on Bus 680

A LL fault is the second most commonly occurring fault in the power system. An SLG fault on bus 680 is replaced by a LL fault between phases A and B. Wave transients that are propagated in phases A and B are approximately equal in magnitude and opposite in polarity. This phenomenon is also observed in the current during a LL fault event. When the waves propagate down the line in both phases, they attenuate and disperse based on the characteristic impedance of two phases. For horizontal line and vertical line configuration, distributed parameters such as inductance and capacitance are the same for all the phases except for the mutual impedance, resulting in small differences in magnitude and dispersion of the waves in both phases.

A fault is applied at 49.14 ms, when the voltage difference between phases is greater. The arrival times of the waves match the estimated values shown in Fig. 4(b). Voltage waves of the selected buses in the taps 1 and 3 are shown in Figs. 12 and 13. A maximum voltage difference of 17.8 kV is observed between the phases at 49.14 ms. An overhead line between the bus 680 and bus 671B is horizontally configured with phase B slightly above phases A and C. Transients in both the phases look very similar in terms of attenuation and dispersion. There is a slight difference in the magnitude observed in Fig. 12 because of the difference in characteristic impedance. As the waves travel away from the fault, magnitude, attenuation and dispersion between phases become distinct, as shown in Fig. 13. The line between bus 632 and bus 645 is vertically configured, resulting in the wave experiencing different distributed characteristic impedances.

D. Overhead Lines with SLG Fault on Bus 645

All the cases discussed so far have the fault on the main feeder. In this case, the fault is assumed in the laterals closer

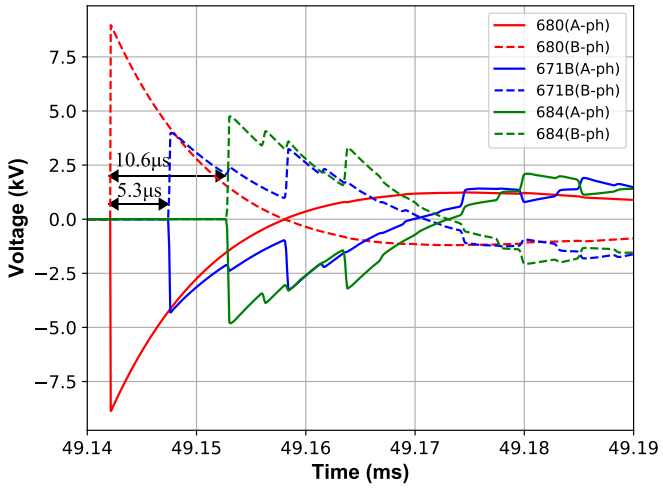

Fig. 12. Voltages in tap 3 buses for a LL Fault

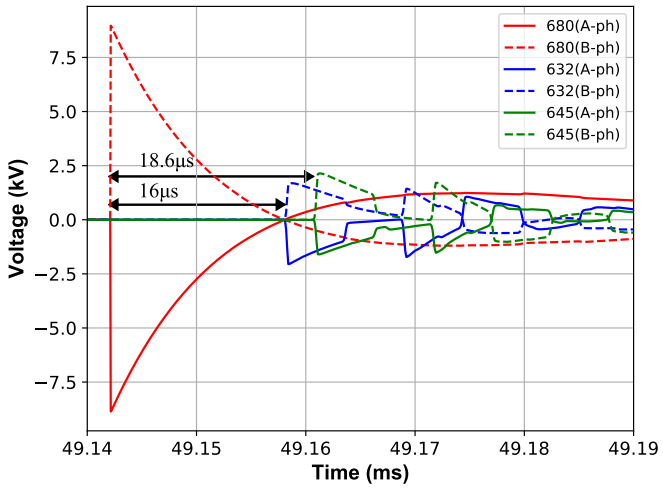

Fig. 13. Voltages in tap 1 for a LL Fault

to the substation at bus 645 in tap 1. When the waves move away from the fault in both directions, one travels down the lateral until it gets reflected, and the other reaches the junction and gets reflected back toward the fault. Voltages in the tap are plotted starting with the faulted bus (see Fig. 14 and 15). The first wave reaches bus 646 after 1.6 μs from the fault. The characteristic impedance of the single phase lines between the buses 645, 646, and 647 is the same. So, the wave launched at 645 attenuates as it travels through two lines unreflected until it reaches bus 647. The waves in the other direction of the fault reach the junction at bus 632 after 2.6 μs.

Voltage signals are used to compare and measure at tap 3 in the test system. Filtered voltages at buses in tap 3 are plotted in Fig. 15. Compared to the signal peak at bus 632, 43% of the wave is recorded at 671B. Waves recorded at junction (632, 671B) stay for a longer duration than buses inside the tap. So, the relays located at the taps can analyze the waves for a fault on main feeder and tap provided that the fault inside the tap is not located far away from the junction.

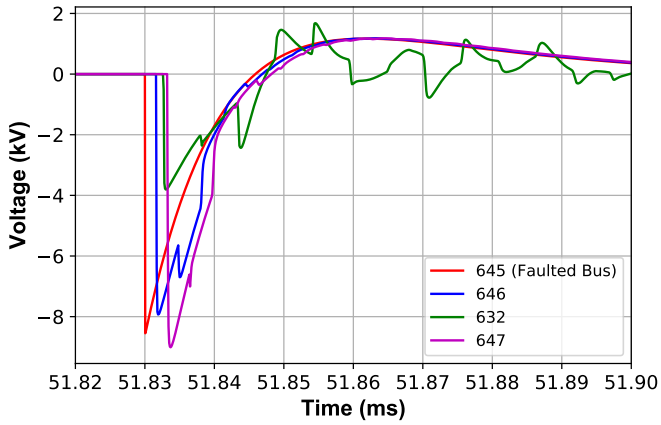

Fig. 14. Voltages in tap 1 for a SLG Fault on bus 645

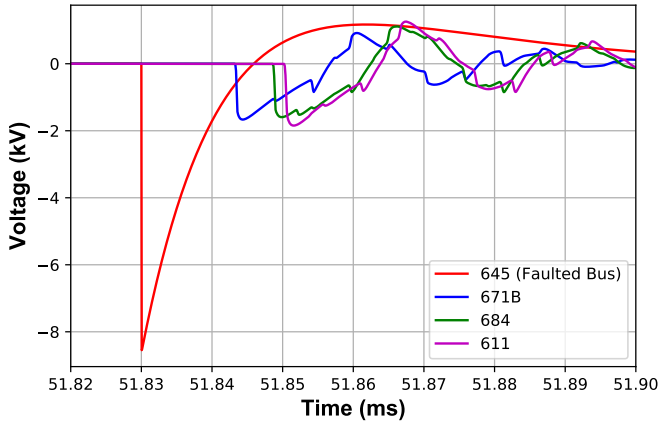

Fig. 15. Voltages in tap 3 for a SLG Fault on bus 645

E. Summary of Results

The simulation results for faults on the main feeder show that two taps beyond faulted bus may not see a measurable second wave reflection from the fault. It is observed from the results that line-to-line fault transients attenuation is less compared to the faults that involve ground. HFWs gets attenuated faster in the lateral due to high resistance of conductors combined with skin effect. This can be observed from the results when the fault location is changed from main feeder to the tap (see subsections (A) and (D)). In the scenario simulated in subsection (B), it is observed that waves travel slower through underground cables compared to the overhead lines.

VI. Conclusion

Limitations of overcurrent, directional, distance and adaptive relaying in the presence of inverter based DER require a novel protection technique that does not depend on fault current magnitudes and direction of power flow. This paper analyzed the application of traveling wave based high-frequency signature for fault detection and location in MV distribution systems. A modified medium voltage IEEE 13-bus test system was presented in this paper to analyze fault generated HFWs. The need for frequency-dependent line modeling to study HFWs was presented and a frequency-dependent line modeling

approach was used to model the modified IEEE 13-bus system. Different fault scenarios of the test system were simulated and results of the EMT simulations were presented. Simulation results indicate that the HFWs can be used as unique signatures of faults and can be used to detect and locate the faults under high DER penetration levels.

ACKNOWLEDGMENT

The authors gratefully acknowledge the support of Guohui Yuan and David Walter of the U.S. Department of Energy Solar Energy Technologies Program, Systems Integration Subprogram, for their valuable advice and funding for this work.

REFERENCES

[1] IEEE Working Group D3, "Impact of Distributed Resources on Distribution Relay Protection," report to the Line Protection Subcommittee of the Power System Relay Committee of The IEEE PES, Aug. 2004.

[2] J. Keller, B. Kroposki, R. Bravo, and S. Robles, "Fault current contribution from single-phase PV inverters," in *2011 37th IEEE Photovoltaic Specialists Conference*, (Seattle, WA, USA), pp. 001822–001826, IEEE, June 2011.

[3] K. Malmedal, B. Kroposki, and P. K. Sen, "Distributed Energy Resources and Renewable Energy in Distribution Systems: Protection Considerations and Penetration Levels," in *2008 IEEE Industry Applications Society Annual Meeting*, (Edmonton, Alberta, Canada), pp. 1–8, IEEE, Oct. 2008.

[4] "IEEE Standard for Interconnection and Interoperability of Distributed Energy Resources with Associated Electric Power Systems Interfaces," *in IEEE Std 1547-2018 (Revision of IEEE Std 1547-2003)*, pp. 1–138, Apr. 2018.

[5] B. Hadzi-Kostova and Z. Styczynski, "Network Protection in Distribution Systems with Dispersed Generation," in *2005/2006 PES TD*, (Dallas, TX, USA), pp. 321–326, IEEE, 2006.

[6] J. Horak and B. Electric, "Directional Overcurrent Relaying (67) Concepts," in *59th Annual Conference for Protective Relay Engineers*, (College Station, TX), p. 13, 2006.

[7] D. Martin, P. Sharma, A. Sinclair, and D. Finney, "Distance protection in distribution systems: How it assists with integrating distributed resources," in *2012 65th Annual Conference for Protective Relay Engineers*, (College Station, TX, USA), pp. 166–177, IEEE, Apr. 2012.

[8] P. Mahat, Z. Chen, and C. L. Bak, "A Simple Adaptive Overcurrent Protection of Distribution Systems With Distributed Generation," *IEEE TRANSACTIONS ON SMART GRID*, vol. 2, no. 3, p. 10, 2011.

[9] S. Ritter, H. Ruttinger, S. Ritter, P. Bretschneider, and D. Westermann, "New approaches for smart grid requirements: Grid protection and optimization of distribution grid operation," in *2011 IEEE Power and Energy Society General Meeting*, (Detroit, MI, USA), pp. 1–7, IEEE, July 2011.

[10] J. Yang and Y. Wang, "Review on protection issues of low-voltage distribution network with multiple powerelectronic-converter-interfaced distribution energy resources," in *International Conference on Renewable Power Generation (RPG 2015)*, (Beijing, China), pp. 6 .–6 ., Institution of Engineering and Technology, 2015.

[11] H. Muda and P. Jena, "Sequence currents based adaptive protection approach for DNs with distributed energy resources," *IET Generation, Transmission & Distribution*, vol. 11, pp. 154–165, Jan. 2017.

[12] J. Gers and C. Viggiano, "Protective relay setting criteria considering DERs and distributed automation," in *13th International Conference on Development in Power System Protection 2016 (DPSP)*, (Edinburgh, UK), pp. 9 .–9 ., Institution of Engineering and Technology, 2016.

[13] B. P. Bhattarai, B. Bak-Jensen, S. Chaudhary, and J. R. Pillai, "An adaptive overcurrent protection in smart distribution grid," in *2015 IEEE Eindhoven PowerTech*, (Eindhoven, Netherlands), pp. 1–6, IEEE, June 2015.

[14] M. Norshahrani, H. Mokhlis, A. H. A. Bakar, J. J. Jamian, and S. Sukumar, "Progress on Protection Strategies to Mitigate the Impact of Renewable Distributed Generation on Distribution Systems," *Energies 2017*, no. 1864, 2017.

[15] E. O. Schweitzer, A. Guzmán, M. V. Mynam, V. Skendzic, B. Kasztenny, and S. Marx, "Locating faults by the traveling waves they launch," in *2014 67th Annual Conference for Protective Relay Engineers*, (College Station, TX), pp. 95–110, IEEE, Apr. 2014.

[16] X. Dong, B. Wang, B. Dominik, and M. Redefern, "Traveling Wave Based Single-Phase-to-Ground Protection Method for Power Distribution System," *CSEE JOURNAL OF POWER AND ENERGY SYSTEMS*, vol. 1, no. 2, p. 8, 2015.

[17] N. Davydova and G. Hug, "Traveling wave based protection for medium voltage grids with distributed generation," in *2017 IEEE Manchester PowerTech*, (Manchester, UK), pp. 1–6, IEEE, 2017.

[18] "Guidelines for Representation of Network Elements When Calculating Transients," 1990.

[19] Neville Watson and Jos Arrillaga, *Power Systems Electromagnetic Transients Simulation*. IET, first ed.

[20] J. R. Marti, "Accurate Modelling of Frequency-Dependent Transmission Lines in Electromagnetic Transient Simulations," *IEEE Transactions on Power Apparatus and Systems*, vol. PAS-101, pp. 147–157, Jan. 1982.

[21] A. Morched, B. Gustavsen, and M. Tartibi, "A universal model for accurate calculation of electromagnetic transients on overhead lines and underground cables," *IEEE Transactions on Power Delivery*, vol. 14, pp. 1032–1038, July 1999.

[22] W. H. Kersting, "Radial distribution test feeders," in *2001 IEEE Power Engineering Society Winter Meeting. Conference Proceedings (Cat. No.01CH37194)*, vol. 2, (Columbus, OH, USA), pp. 908–912, IEEE, 2001.

[23] "Distribution Conductor Clearances and Span Limitations," July 2003.